Opto-Electronics Review 29 (2021) 13-32

PAN POLISH ACADEMY OF SCIENCES

Opto-Electronics Review

journal homepage: http://journals.pan.pl/opelre

Recent advances in mode converters for a mode division multiplex transmission system

A. K. Memon and K. X. Chen*

School of Optoelectronic Science and Engineering, University of Electronic Science and Technology of China, Chengdu 610054, P. R. China

Article info

Article history:
Received 15 Dec. 2020
Received in revised form 7 Mar. 2021
Accepted 8 Mar. 2021

Keywords:
Integrated optical device, mode converter, mode division multiplex, optical waveguide.

Abstract

Adopting mode division multiplex (MDM) technology as the next frontier for optical fiber communication and on-chip optical interconnection systems is becoming very promising because of those remarkable experimental results based on MDM technology to enhance capacity of optical transmission and, hence, making MDM technology an attractive research field. Consequently, in recent years the large number of new optical devices used to control modes, for example, mode converters, mode filters, mode (de)multiplexers, and mode-selective switches, have been developed for MDM applications. This paper presents a review on the recent advances on mode converters, a key component usually used to convert a fundamental mode into a selected high-order mode, and vice versa, at the transmitting and receiving ends in the MDM transmission system. This review focuses on the mode converters based on planar lightwave circuit (PLC) technology and various PLC-based mode converters applied to the above two systems and realized with different materials, structures, and technologies. The basic principles and performances of these mode converters are summarized.

1. Introduction

Data traffic in optical communication systems has increased rapidly in the last decade [1,2]. According to the latest report published by CISCO, there will be a need for a high transmission capacity up to 400 Exa (1018) bytes per month in 2022 to deal with the global internet traffic [2], as depicted in Fig. 1. This demand undoubtedly impels telecommunication industry to implement the next generation optical communications system to cope with hungry bandwidth applications [3,4]. To this end, different technologies have been explored to meet the rapid growth in data traffic [5-8] in which multiplexing technology plays a crucial role and has been studied for several decades [5,9-11].

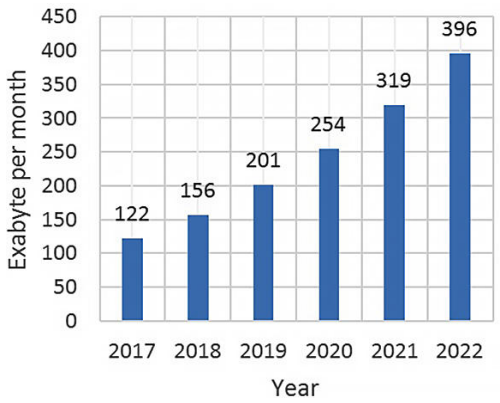

Fig. 1. CISCO survey for the global internet traffic [2].

Multiplexing technology enhances the transmission capacity of optical fibers by employing parallelism in all physical dimensions of electromagnetic waves, including time, quadrature, polarization, frequency, and space [3-5,9]. Nowadays, commercially deployed optical core networks have taken full advantage of time, quadrature, polarization, and frequency. Undoubtedly, the much enjoyed information era owes a lot to the dense wavelength division multiplexing (DWDM) technology which empowers a single-mode optical fiber to transmit an enormous number of close wavelength channels at high data rates over a long distance [3,4,9]. However, with a consistent and rapid growth of the network traffic, transmission capacity of the DWDM framework is rapidly approaching its most

*Corresponding author at: chenkx@uestc.edu.cn

https://doi.org/10.24425/opelre.2021.135825.
1896-3757/ Association of Polish Electrical Engineers (SEP) and Polish Academic of Sciences (PAS). Published by PAS

extreme point of a single-mode fiber bandwidth confinement, which is estimated at ~100–200 Tbit/s and known as an optical networks capacity crunch [3]. To address these issues, space division multiplexing (SDM) [7-9] and mode division multiplex (MDM) [10-13] have been proposed and developed worldwide. SDM depends on more cores in a single glass strand, named as a multicore fiber (MCF), while MDM employs different spatial modes or mode groups in a few-mode fiber (FMF) to convey signals in parallel. These two new technologies have been demonstrated experimentally by researchers around the world [13-16]. Furthermore, combining effectively these two technologies to achieve ultra-high transmission capacities of an optical fiber communication system has also been demonstrated [15,16], including a record fiber capacity of 10.16 peta-b/s [15].

Besides, being used in the optical fiber communication system, MDM technology has also been introduced into an on-chip optical interconnection system to enhance transmission capacity [17,18] and remarkable advances have also been achieved [19-21].

These significant experimental results make MDM a promising technology and an attractive research field. Consequently, in recent years the large number of new optical devices used to control modes, for example, mode converters, mode filters, mode (de)multiplexers, and mode-selective switches, has been developed for MDM applications. This paper presents a review on the recent advances on mode converters, the key component usually used to convert the fundamental mode into a selected high-order mode, and vice versa, at transmitting and receiving ends in the MDM transmission system [14,15]. The review is focused on the mode converters based on a planar lightwave circuit (PLC) technology and applied in both optical fiber communication and on-chip interconnection systems. Two application scenarios are not deliberately distinguished. Various PLC-based mode converters were used in the above systems and realized with different materials, structures, and technologies which are presented in the article, as well as the basic principles and performances of these mode converters which are summarized, aiming to give the reader a comprehensive and broad view of the field.

2. Mode conversion in MDM system

Considering the fact that many existing optical devices are intended for a fundamental mode operation, the mode conversion is critical for the use of these devices in the MDM system. As an optical device, insertion loss (IL) is one of the key parameters to evaluate the performance of a mode converter. IL includes a waveguide propagation loss and a coupling loss between the fiber and the chip, where the propagation loss in some literature is also called an on-chip IL and, especially, for a mode converter comprised of mode conversion loss (MCL), which is an important parameter to evaluate the mode conversion mechanisms, and other losses such as absorption loss and scattering loss. Another key parameter for a mode converter is mode conversion efficiency (MCE) which is defined as the power ratio of the target (or converted) mode to the initial mode. The mode conversion performance of a mode converter can also be characterized by its mode crosstalk (MCT) or mode extinction ratio (MER). MCT is defined as the power ratio of the residual mode to the target (or converted) mode. MER is defined as the power ratio of the target (or converted) mode to the residual mode. Obviously, MER = −MCT (in dB), and MCE and MCT can be derived from each other when transmission and conversion losses are neglected. In addition to the above key parameters, bandwidth is also an important parameter of a mode converter in view of the prediction that future MDM networks should be compatible with the existing DWDM technology.

Nowadays, various types of mode converters based on optical fibers [14], bulk-optic components [15,16], and PLC technology have been proposed [17-87]. Among them, PLC technology offers more adaptability in the choice of materials and physical principles, as well as the flexibility in design and fabrication processes, and it allows to create compact, fiber-compatible, and monolithically integrated devices. In this paper, various PLC-based mode converters employing different structures are presented, including Mach-Zehnder interferometers (MZIs) and the like, multimode interference (MMI) couplers, asymmetric directional couplers (ADCs), long period gratings (LPGs), Bragg gratings (BGs), Y-junctions, ring, dielectric metasurface structures, and tapered, irregular, oval waveguides, as well as other special waveguides. It should be pointed out that some mode converters, such as ADC-based and Y-junction-based converters, have also the ability to (de)multiplex different modes, but here they still have been considered as mode converters. According to their respective operation principle, these aforementioned mode converters can be categorized roughly into three types: reconstitution type (or beam shaping type), coupling type, and evolution type. The following section will review them one by one. Note that the name and the order of the involved modes in this review follow those in the respective works.

3. Three types of mode converters

3.1 Mode reconstitution type

Operation principle of the mode reconstitution converters is based on the manipulation of the phase relationship of intra-mode with three functional components used for mode decomposition, phase shift, and mode reconstitution. Nowadays, this type of mode converters has been demonstrated by employing MZI [22-29,43], MMI couplers [30,31], and special waveguides with well-designed index distribution [32-42]. Their key performances have been summarized in Table 1 in the Appendix.

MZI-based mode converters offer advantages of simple structure, easy design, low IL, and high MCE. In 2006 Y. Y. Huang *et al.* [22] proposed an ultra-compact mode converter based on an unbalanced MZI configuration to achieve the conversion between the TEM_{00} and TEM_{01} modes. The proposed device dictates that the input TEM_{00} mode split in half by a Y-splitter to achieve phase difference between two beams, which then is recombined at another Y-junction with a broadened output waveguide to produce the first-order mode. Their simulated results achieve the MCE of 94% at a 1550 nm wavelength. Their

fabricated device with InP has an ultracompact footprint of less than 18 μm by 3 μm and achieves a low MCL of 0.4 dB. In 2015, B. B. Oner *et al.* [23] also proposed a similar unbalanced MZI-based mode converter using equal arm lengths but different cross-sectional areas to achieve a large bandwidth mode-order conversion from the fundamental to the higher odd mode. However, no experimental demonstration was presented in this work.

In the above works, Y-junction was used to decompose the input modes which usually leads to a device large footprint. Considering that an MMI coupler has advantages of compact size, low loss, and relatively large optical bandwidth, it has also been proposed as a mode decomposer to structure a compact mode converter [24-29]. In 2012 T. Uematsu *et al.* [24] proposed a two-mode multi/demultiplexer using an MMI coupler to decompose the input modes. Their designed device for the implementation of a conversion between the fundamental and the first-order mode achieves a theoretical MCE of around 90% over C-band. Subsequently, several similar mode converters employing a different waveguide structure to realize the required phase shift were proposed or demonstrated. In Ref. 25, L. S Han *et al.* proposed a compact mode converter by employing a tilted joint to provide the phase difference required by the mode conversion between the fundamental and the first-order mode. The proposed device is as small as 39.54 μm and obtains an MCT lower than −28 dB, as well asan on-chip IL of 1.0 dB. In Ref. 26, F. Guo *et al.* introduced a waveguide section with a varying thickness to precisely control the phase shift so as to achieve a 100% MCE. Their well-designed device can achieve an on-chip IL less than 1.2 dB and an MCT less than −18.4 dB over C-band for the TE_0-TE_1 conversion, while their experimental mode converter fabricated with InP exhibits that averaging excess losses of TE_0 mode to TE_1 mode are of around −8 dB in the wavelength range from 1520 nm to 1600 nm. But no experimental MCE is presented. AA broadband and low crosstalk mode converter fabricated with SOI was demonstrated by D. Chack *et al.* in 2020 [27] showing that MCT between the TE_0 and TE_1 modes is less than −20 dB over 1520–1580nm. In Ref. 28, H. D. T. Linh *et al.* proposed an arbitrary mode converter based on two symmetric 1 × 4 Y-junction couplers connected back-to-back with a 4 × 4 MMI. Butterfly-shaped phase shifters with different waveguide widths were placed at the input and output of an MMI coupler to achieve the required phase shift. The proposed device is capable of an implementation of arbitrary conversion from TE_i to TE_j (i, j = 0, 1, 2, 3 - as modes example see the picture in Table 2) modes with theoretical MCEs larger than 98% and MCTs smaller than −30 dB in the wavelength range from 1530 nm to 1565 nm. In Ref. 29, D. González-Andrade proposed an ultra-broadband two-mode converter and (de)multiplexer based on a sub-wavelength engineered MMI (SWG-MMI), a 90º-phase shifter, and a symmetric Y-junction. They realized a 90º-phase shift by introducing two trapezoidal tapers in back-to-back in the upper arm and a straight waveguide in the lower arm. The proposed device is of 36 μm × 3.7 μm and exhibits a theoretical MCT less than −20 dB, and an on-chip IL less than 0.84 dB in the wavelength range of 1400 nm to 1700 nm.

Employing a single MMI coupler to restructure the intensity profile and the phase relation within the mode via multimode interference and, hence realize the mode conversion has been proposed [30,31]. The proposed mode converters inherit the strength of compact and broadband of the MMI couplers. In 1998 J. Leuthold *et al.* [30] proposed and demonstrated two MMI configurations, named respectively as 50% and 66% type according to their respective theoretical MCE for achievement of the mode conversion between the fundamental and the transversal first-order mode. Both types of the mode converters they fabricated with InGaAsP/InP exhibit excess losses (i.e., MCL) below 0.3 dB at a 1500-nm wavelength, which means a high MCE. In 2016 F. Guo *et al.* [31] also demonstrated the above two types of MMI-based TE_0-TE_1 mode converters on an InP substrate, both achieved the relative ILs less than 3.9 dB and 1 dB, respectively, in the wavelength range of 1280–1320 nm.

Mode converters employing the special waveguides with a well-designed index distribution to restructure the intensity profile and the phase relation within the mode have also been proposed [32-42]. This type of mode converter is usually implemented with a high-contrast-index materials platform, especially with SOI due to its quite high index difference and mature waveguide fabrication processes. The desired index distribution is usually achieved by introducing irregular waveguide core [32-34], inlaid dielectric substrip waveguides [35,36], sub-wavelength grating [37], shallowly or deeply etched structure [38-41], and metasurface [62]. In 2006 H. -T. Chen and K. J. Webb [32] proposed a novel mode converter in which an irregular SOI waveguide with a stepwise variation in width was used to scatter the input light and then restructure its intensity and phase profile. Their well-designed mode converter using a multi-resolution optimization procedure with a three-dimensional vector finite element forward solver for the conversion between the fundamental and the first-order mode exhibits a theoretical MCE of 94.2%. In 2015, similar mode converters for the TE_1-TE_0, TE_2-TE_0, TE_3-TE_0, TE_2-TE_1, TE_3-TE_1, and TE_3-TE_2 conversions have also been proposed and demonstrated theoretically by D. Chen *et al.* [33] on a SOI platform with average conversion efficiencies of 98.6%, 98.8%, 97.5%, 97.3%, 96.2%, and 96.5%, respectively over 1520–1580 nm. Afterwards, Z. Y. Chen *et al.* further simplified a complicated irregular waveguide core in Ref. 33 into an oval waveguide in 2018 [34]. The oval waveguide used in this work has two symmetric smooth boundaries shaped like semi-ellipse, resulting in an optical phase difference between the path along the semi-major of the oval (path 1) and the path along the boundary (path 2). Their fabricated device with SOI for the implementation of the conversion from the TE_0 mode to the TE_2 and TE_4 modes obtains an MCT of −19.0 dB and −16.0 dB, respectively, over 1520–1580 nm. Disadvantage of this converter is that it works only for even modes due to their structural symmetry.

Employing inlaid dielectric substrip waveguides to obtain mode decomposition and phase shift for a desired mode conversion has also been proposed [35,36]. In 2018 D. F. Zhu *et al.* [35] proposed a novel mode converter by introducing a high refractive index material inlaid in a SOI

multimode waveguide for the implementation of the TE_0-TE_1 and TM_0-TM_1 conversions. Their proposed mode converter has a quite small footprint of 0.95 × 1.5 μm^2. The calculated transmittance (i.e., MCE) of TE_0-TE_1, TE_1-TE_0, TM_0-TM_1, and TM_1-TM_0 modes are of 89.5%, 90.6%, 88.1%, and 88.9% at 1550 nm, respectively, and larger than 97% for all above conversion over 1500–1600 nm. In 2019 B. E. Aby-Elmaaty *et al.* [36] proposed a mode converter based on silica substrip waveguides inlaid in a SOI waveguide. The proposed device can convert the fundamental mode into any higher-order mode. Their fabricated two devices for the TE_0-TE_1 and TE_0-TE_2 conversions exhibit that the on-chip ILs of the TE_1 and TE_2 modes are of −2.09 dB and −1.37 dB, the MCTs are of −13.41 dB and −12.63 dB, respectively.

In 2019 Z. Cheng *et al.* [37] proposed three-mode converters using a sub-wavelength grating to modulate the index distribution on a SOI substrate for the conversion of the TE_0 mode to the TE_1, TE_2, and TE_3 modes. Three-mode converters they designed are of 8.72 μm, 4.98 μm, and 14.54 μm, and they exhibit theoretical MCEs larger than 94.4%, 95.7%, and 83.7%, MCTs less than −15.33 dB, −17.36 dB, and 15.65 dB, respectively, over 1520–1580 nm.

Shallowly or deeply etched structure formed on the waveguide surface has also been employed to modulate the index distribution for the mode conversion. In 2017, W. Ye [38] proposed a TE_0-like to a TE_1-like mode-order converter based on silicon nanowires with two cascaded fully etched trenches. In this work, two trenches have a horizontal mirror symmetry, resulting in different propagation constants and spatial distributions of the mode filed in the slot nanowire, and, hence, effectively converting the TE_0-like into the TE_1-like mode. The proposed device has a footprint as small as 0.8 × 5.3 μm^2 and exhibits a theoretical transmittance larger than 0.95 over the wide wavelength range of 1420 nm to 1620 nm. In 2019 L. P. Liu *et al.* [39] proposed a compact TM_0-TM_2 mode converter based on shallowly etched rhombus and triangle, where the rhombus etching part is used to decompose the input fundamental TM_0 mode and the two triangle etching parts are employed to introduce a phase difference of π between adjacent beams. Their simulation results show a high MCE of ~94%, a low MCT of < −15 dB, and a low on-chip IL over 1458–1560 nm. Also in 2019 L. J. Hao *et al.* [40] proposed a new type of TE polarized mode-order converter based on a deeply-etched polygonal slot on a SOI waveguide. In this work, a high-contrast index modulation introduced by the slot leads to a multimode interference in the slot and, hence, an efficient mode conversion. Their well-designed devices based on tilted, bi-tilted, and tri-tilted slots for the TE_0-TE_1 and TE_0-TE_2 conversions exhibit the MCEs of 97.6% and 99.4%, the MCTs of −27.3 dB and −26.4 dB, respectively, over the broad wavelength range from 1500 nm to 1600 nm. Similarly, by introducing dielectric slots, an ultra-compact mode-order converter based on a SOI waveguide has also been proposed and demonstrated by Y. T. Zhao *et al.* in 2020 [41]. In this work, the slot waveguide plays the roles of a beam splitter and a taper phase shifter. Their fabricated devices for the TE_0-TE_1 conversion exhibit the MCT less than −6.3 dB and the on-chip IL less than 1.2 dB from 1520 nm to 1570 nm.

Referring to the concept of a silicon planar meta-surface, in 2019 H. Jia *et al.* [42] proposed a dual-polarization mode-order converter. Functional region of the proposed device consists of multiple subwavelength subunits and a mode conversion is achieved by controlling materials or duty cycles of each subunit. Their fabricated prototype, which has a footprint of 4 μm × 1.6 μm, can realize the TE_0-TE_1 and TM_0-TM_1 conversions simultaneously with the on-chip ILs from 1.0 to 2.3 dB and 0.9 to 1.4 dB, and the MCTs lower than −13.7 dB and −11.8 dB for the TE and TM polarizations, respectively, within the wavelength range of 1525–1565 nm.

All the above structures have a common drawback, i.e., fixed mode conversion, which is disadvantageous to the implementation of reconfigurable and flexible MDM systems. To overcome this issue, an electro-optic mode converter based on an optical waveguide MZI has also been proposed by M. R. Zhang *et al.* in 2016 [43]. Their typical fabricated device with lithium niobate (LN), which is of a total length of ~24 mm, can achieve a switchable mode conversion between the TE_{11} and TE_{21} modes with the MCE of ~35 dB and a 20-dB bandwidth of ~12 nm at the wavelength of 1552 nm, when driven at a voltage of 1.7 V at 26°C. High performance can also be obtained at any wavelength in the C + L band with a driving voltage varying by no more than 3 V.

To sum up, MZI-based mode converters are capable of achieving a quite large MCE and a quite low MCT, but with a large footprint, usually. MMI-based mode converters can achieve a compact size, but a low MCE and a large MCT. These mode converters based on special waveguide structures are not only more compact but also with the capability of achieving a large MCE and a low MCT, even if their performances are slightly inferior to the MZI-based mode converters. In addition, as for the implementation of reconfigurable mode converters by introducing the electro-optic or thermo-optic effect, the MZI configuration is more suitable because it has two arms that can be controlled independently.

3.2 Mode coupling type

Operation principle of the mode coupling converters is based on the coupling between the fundamental and the selected high-order mode under the condition of their phase matching. Such a mode coupling is usually achieved by using ADC, [44-57,73,78], ring [58,59], LPG [60-65,72,74,75], BG [66,67], dielectric metasurface structure [68-70], and grating-assisted coupler [71], and so on. Their key performances have been summarized in Table 2 in the Appendix.

In 2013 N. Hanzawa *et al.* [44] proposed firstly a LP_{01}-LP_{11} mode converter based on ADC formed with two planar parallel waveguides with a different width. In this work, by designing suitable widths of the two waveguides to match the effective index of the LP_{11} mode in waveguide 1 to that of the LP_{01} mode in waveguide 2, the LP_{01} from port 1 propagated directly to the output port 3 while LP_{01} from port 2 is converted to the LP_{11} mode propagated to the output port 3 (as modes example see the picture in Table 2). Their fabricated device with silica exhibited MER from the LP_{01} to LP_{11} modes larger than 20 dB between 1500 and

1620 nm and MER from the LP_{11} to LP_{01} modes larger than 15 dB over the C-band with an IL less than 1.3 dB. Subsequently, to implement (de)multiplexing of the LP_{11b} mode, in 2014 K. Saitoh *et al.* [45] further proposed and demonstrated a mode rotator to convert the LP_{11a} to LP_{11b} modes (as modes example see picture in Table 2). Their proposed device is composed of a straight waveguide with a trench. Their fabricated device with silica achieves the MCE larger than 90% over the wide wavelength range from 1450 nm to 1650 nm. Afterwards, researchers from the same group combined their proposed mode rotator and an ADC-based mode converter to demonstrate the mode conversions from the LP_{01} to the LP_{11b}, LP_{21a}, LP_{21b}, LP_{02}, and vice versa successively [46-48]. Especially, K. Saitoh *et al.* [48] demonstrated a six-mode (de)multiplexer by employing six ADCs and a two-mode rotator to achieve the desired mode conversions from the LP_{01} to the LP_{11a}, LP_{11b}, LP_{21a}, LP_{21b}, and LP_{02}. The near field patterns measured at the MUX port show clear mode patterns of these six desired modes, but no experimental MCEs were presented. Note that in this work two well-designed tapered waveguides are used to convert the E_{31} and E_{13} modes into the LP_{02} and LP_{21b} modes, respectively.

In the aforementioned works, due to the limitation of mode symmetries, the mode conversion between the LP_{01} and the LP_{11b} was achieved indirectly, i.e., with the help of a mode rotator which augments the device complexity. To overcome this issue, in 2014 N. Riesen *et al.* [49] proposed and demonstrated three-dimensional (3D) integrated mode couplers for a direct conversion of the LP_{01} and LP_{11b} modes, firstly. Their proposed mode converter consists of horizontal and vertical couplers formed with three cores fabricated using the femtosecond laser direct-write technique, where the horizontal coupler is responsible for the conversion between the LP_{01} and LP_{11a} modes, while the vertical coupler is responsible for the conversion between the LP_{01} and LP_{11b} modes. Their experimental mode converter shows the MCEs from 53% to 68% and 80% to 99%, and the MERs from 26 dB to 32 dB and from 35 dB to 37 dB for the LP_{01}-LP_{11a} and LP_{01}-LP_{11b} conversions, respectively, both with an IL lower than ~1 dB over 1500–1580 nm. Subsequently in 2015 J. L. Dong *et al.* [50] also proposed a similar 3D waveguide mode multiplexer formed with horizontal and vertical ADCs to achieve the LP_{01}-LP_{11a} and LP_{01}-LP_{11b} conversions. Their proposed device consists of two dissimilar single-mode core waveguides placed along with a central three-mode rectangular waveguide in the horizontal and vertical direction, respectively. With this structure, the LP_{11a} and LP_{11b} modes of the central waveguide can be coupled into the LP_{01} modes of the horizontal and vertical waveguides, respectively. Their typical fabricated device with optical polymer materials, with a length of 9 mm, shows MCEs from 91% to 99%, MCTs from −23.2 dB to −14.6 dB, and an IL of 10 dB, and these results are weakly sensitive to the polarization state of light and, also, insensitive to temperature. Further in 2016, F. K. Wei *et al.* [51] also experimentally demonstrated a 3D mode converter based on a vertical polymer ADC. Their fabricated device for the conversion of LP_{01} and LP_{21a} exhibits a maximum MCE of 98.7% at 1550 nm and a 10-dB bandwidth of ~40 nm. In 2018, Q. Huang *et al.* [52] further developed a 3D mode converter to a higher level by the design and fabrication of a 3D mode (de)multiplexer based on cascaded ADCs to convert the E_{21}, E_{12}, E_{22}, E_{31}, and E_{13} modes into the E_{11} mode, and vice versa (as modes example see the picture in Table 2). Their typical fabricated device, with a length of 29 mm, achieves MCEs varying from 62% to 90% and MCTs from −28.2 dB to −11.6 dB in the wavelength range from 1530 nm to 1565 nm with a weak polarization dependence.

Although a vertical DC can be designed to couple between two arbitrary spatial modes, it requires a multi-layer structure and an accurate alignment of waveguides in the vertical direction which complicates the fabrication process. In view of this, in 2017 W. K. Zhao *et al.* [53] proposed and demonstrated a horizontal DC formed with two parallel waveguides of different heights to achieve directly a mode conversion between the LP_{01} and LP_{11b} modes. By breaking the symmetry in both horizontal and vertical direction, their proposed DC can achieve the coupling between any two spatial modes of a few-mode waveguide. Their typical fabricated device for the conversion between the LP_{01} and LP_{11b} modes shows the MCE higher than 95% in the wavelength range from 1530 nm to 1560 nm. After that, in 2019 W. K. Zhao *et al.* [54] further developed a five-mode (de)multiplexer with a polymer material to achieve the conversions from E_{11} to E_{12}, E_{21}, E_{31}, and E_{22} modes with the same idea. In this work, they further introduced a tapered DC to enlarge the operation bandwidth of the device. Their typical fabricated device is 2.1-cm long and shows the MCEs larger than ~94.5% for each DC over the C + L band with a weak polarization dependence.

Mode conversion using an ADC formed with a hybrid plasmonic waveguide and a silicon nanowire waveguide was also proposed by M. Yin *et al.* [55] in 2014. Theoretical MCE of 99.2% for the conversion of the TE_0 and TE_1 modes with a coupling length of 13.6 μm is achieved at 1550 nm. In addition, by cascading horizontal ADCs, an 8-channel silicon mode (de)multiplexer manipulating mode conversions from TE_0 to TE_1, TE_2, and TE_3 and TM_0 to TM_1, TM_2, and TM_3 was also demonstrated by J. Wang *et al* [56] in 2014. Their fabricated device with SOI shows the MCTs from −11 dB to −20 dB for all mode conversions in the wavelength range from 1520 to 1610 nm.

To improve the fabrication tolerances of silicon ADC mode converters, in 2017 D. Garcia-Rodriguez *et al.* [57] proposed a high-performance ADC mode converter based on optimized dimensions. Their theoretical results show the MCE of 97% and the MCT of 23.4 dB over 1540–1560 nm. However, their experimental results only achieve the MCE of 90% at 1550 nm and a 20 -nm bandwidth with the MCE higher than 84%.

Mode converter using a ring resonator has also been proposed and demonstrated [58,59]. In 2013 L. -W. Luo *et al.* [58] proposed a low MCT device using an add-drop silicon ring resonators array. In this work, a bus waveguide was tapered successively to different widths to selectively phase-match different bus waveguide modes to a ring waveguide mode. Such a device layout forms one DC and two ADCs which are used to convert the TE_0, TE_1, and TE_2 modes in a bus waveguide into the TE_0 in three ring resonators, respectively. Their fabricated device shows a

low MCT less than −20 dB at 1547.4 nm. In 2015 Y. Yu *et al.* [59] proposed and demonstrated experimentally an on-chip polarization-controlled mode converter using a ring resonator. By selecting either horizontal or vertical linear polarization at an input single-mode fiber, their proposed device can either convert the input LP_{01} mode to the LP_{11} mode or maintain the LP_{01} mode in the output FMF over the C-band. The measured mode profiles from the FMF output verify successfully the mode conversion with an MCT equal to −12 dB.

Mode converters employing LPG [60-65] or BG [66,67] to achieve the coupling conversion between the fundamental mode and the desired mode have also been proposed. In 2015 Y. Yang *et al.* [60] fabricated a surface-corrugated LPG on a polymer waveguide for the conversion between the LP_{01} and the LP_{11b} mode. Their typical fabricated device shows the MCE of ~99% at 1536 nm with a bandwidth of 4 nm and a temperature sensitivity of 3.5 nm/°C which allows the device operation wavelength to be tuned over the C + L band with a temperature control <30°C. Similarly, to achieve the mode conversion between the LP_{01} and LP_{11a} modes, in 2015, W. Jin *et al.* [61] also proposed and fabricated a mode converter employing a sidewall-corrugated LPG. Their fabricated device shows a higher MCE of 99% at 1600 nm with a bandwidth of 20 nm and a thermal tuning sensitivity of 4.1 nm/°C over the S + C + L band. Subsequently, in 2016 W. Jin *et al.* [62] further proposed and demonstrated two types of mode converters with polymer materials by cascading the surface- and the sidewall-corrugated LPG. The modes symmetry properties dictate that the surface- and the sidewall-corrugated LPGs allow a specific mode conversion which is fully exploited to design their proposed two types of mode converters. The measured results show that the first type of mode converter, which allows the conversion among the LP_{01}, LP_{11b}, and LP_{11a} modes in a cyclic manner, achieves a maximum MCE of 94% at 1540 nm, while the second type of mode converter, which allows the conversion between the LP_{01} and LP_{21a} modes, achieves a maximum MCE higher than 90% at 1550 nm.

To enlarge the bandwidth of LPG-based mode converters so that they match the DWDM system requirement, in 2017 W. Wang *et al.* [63] proposed and demonstrated an ultra-broadband mode converter using a length-apodized LPG. Their fabricated LP_{01}-LP_{11b} (LP_{01}-LP_{11a}) mode converter, which used a 3-section length-apodized surface (sidewall) LPG formed along a polymer optical waveguide, obtains the MCE higher than 99% over a bandwidth of ~120 (~150) nm, or the MCE higher than 90% over a bandwidth of ~180 (~300) nm. Further, in 2019, W. K. Zhao *et al.* [64] proposed and demonstrated a novel and ultra-short embedded LPG for implementing a broadband mode conversion. In this work, the embedded LPG features an ultra-short length and a wide bandwidth is formed by locating the perturbation inside the waveguide where the two coupling modes have the largest field overlap. In addition, the internal disturbance implementation also provides a versatile mechanism for manipulating the phase-matching curve of the proposed grating by engineering the rectangle perturbation aspect ratio which further helps to increase the proposed grating bandwidth. Their fabricated device with polymer materials, which contains only two periods with a grating length of 824 μm, achieves MCEs larger than 98.2% over the C + L band. The advantage of the proposed embedded LPG is that its length is only of a quarter of the length of the standard sidewall or surface LPG but with a wider bandwidth.

To extend the LPG-based mode converters for the conversion of any nondegenerate modes of a waveguide, regardless of their symmetry properties, in 2018 W. Jin *et al.* [65] proposed a 3D LPG mode converter with a controllable grating width and depth which can be formed at any chosen position on the waveguide core surface. Using a negative tone photoresist as a waveguide material, they fabricated several mode converters with their proposed structure, including the E_{11}-E_{12}, E_{11}-E_{22}, and TE_{21}-E_{12} mode converters, to show the flexibility of the proposed 3D grating structure. The experimental MCEs achieved with these three mode converters are higher than 98%, 95%, and 94% at their respective resonance wavelengths of 1545 nm, 1575 nm, and 1550 nm.

Beside LPG, BG has also been proposed to implement mode conversion. In 2005, C. M. Greiner *et al.* [66] experimentally demonstrated a novel grating which only produced reflection with a mode conversion in a two-mode waveguide. Mode conversion is due to the fact that the index perturbation used in this work has a π-phase shift with respect to the lateral symmetric axis for the waveguide modes. Their fabricated device with a silica waveguide achieves a mode-converting reflection (i.e., MCE) of 99% from the even (i.e., fundamental) mode to the odd (i.e., first higher-order) mode, and vice versa, for both TE and TM polarizations. Using the same principle, in 2019, R. L. Xiao *et al.* [67] also proposed an on-chip mode converter which can achieve a forward conversion between two guided modes via two cascaded Bragg reflection processes. Their theoretical and simulation results show that forward mode conversions from TE_1 to TE_0 and to TE_2, with adjustable bandwidth and central wavelength can be realized by optimizing grating parameters. Their fabricated proof-of-principle device with SOI achieves the conversion from the TE_2 to TE_0 and to TE_1 with the MCT of –7 dB.

Mode converters using a dielectric metasurface structure in silicon to achieve the coupling between the desired modes have also been proposed. In 2019 H. W. Wang *et al.* [68] proposed and demonstrated a compact silicon waveguide mode converter based on an all-dielectric metasurface structure with a tilted subwavelength periodic perturbation. Their fabricated two proof-of-principle devices can convert the TE_0 mode to the TE_1 and the TE_2 mode with coupling lengths of 5.75 and 6.736 μm, the MCL lower than 1 dB and 0.5 dB, the MCT lower than −10 dB in the wavelength range of 1542–1563 nm and 1545–1563 nm, respectively. In 2014 D. Ohana and U. Levy [69] proposed a novel mode converter in a silicon waveguide based on a graded index co-directional grating coupler featuring a periodic variation in its refractive index along the propagation direction and a graded index profile along the transverse direction. The graded index profile, which accounts for maximizing the coupling strength by increasing the field overlap, is realized by using the effective medium concept in which a subwavelength grating with a variable duty cycle is etched into the silicon waveguide. At 1550 nm wavelength, their designed

TM_0-TM_1, TM_0-TM_2, and TM_0-TM_3 mode converters with lengths of 20, 19, and 18.5 μm exhibit total transmissions (MCEs) of 97%, 97%, and 96%, the MCTs of −27.9 dB, −45.1 dB and −23.9 dB. Afterwards, in 2016, D. Ohana and U. Levy *et al.* [70] further demonstrated experimentally their proposed nanoscale mode converter in Ref. 69, the device they fabricated with SOI achieves the conversion between the LP_{01} and the LP_{11} mode with a measured mode purity of ~95%, in excellent agreement with theoretical results in Ref. 69.

Using a grating-assisted coupler to implement mode conversion has also been proposed by H. Y. Qiu *et al.* [71] in 2011. The device designed with SOI achieves the conversion from the fundamental mode of the access waveguides to the 1st, 2nd, and 3rd modes of the bus waveguide, and vice versa, the corresponding coupling lengths are of 250 μm, 150 μm, and 90 μm, respectively. MCTs of demultiplexers of the channels 1 (1st mode), 2 (2nd mode), and 3 (3rd mode) are of −22.6 dB, −26.8 dB and −30.3 dB, respectively. Compared with the conventional ADC, the grating-assisted coupler offers the advantage that the mode coupling can be flexibly controlled by designing the grating period at the phase-matching condition. Especially, high selectivity for the coupling wavelength makes it easy to incorporate the DWDM and MDM technologies into the same device.

Beside the above fixed mode converters, reconfigurable or switchable mode conversion devices based on the thermo-optic and electro-optic effects have also been proposed [72-76]. In 2018, W. K. Zhao *et al.* [72] proposed and demonstrated a thermally induced LPG integrated with an asymmetric Y-junction to achieve a reconfigurable mode conversion. In this work, a periodic heating electrode deposited on the two-mode waveguide induces the LPG designed for the E_{11}-E_{21} mode conversion by applying electric power to the electrodes. Thus, the mode conversion can be switched by controlling the electric power applied to the heater. Their typical fabricated device with polymer material shows a mode selectivity higher than 12 dB over the C + L band at a switching power of 198 mW which means a high MCE. In 2018, X. Z. Zi *et al.* [73] proposed a simple thermo-optic mode-selective switch based on an asymmetric directional coupler. The proposed device consists of a two-mode waveguide, a single-mode waveguide, and two heating electrodes deposited on the two waveguides, respectively. With such a device layout, mode conversion between the LP_{11a} mode in the two-mode waveguide and the LP_{01} mode in the single-mode waveguide can be switched by controlling the electric power applied to the single-mode waveguide electrode. The device they fabricated with polymer materials is 16.5-mm long and shows the MER larger than 10 dB, switching powers of 52 mW, and 109 mW in the C-band for both modes, respectively, as well as the corresponding switching times are of 300 μs and 400 μs.

Considering the fact that the switching speed of thermo-optic devices is slow, reconfigurable or switchable mode conversion devices based on the electro-optic effect have also been proposed. In 2015 W. Jin *et al.* [74] proposed and demonstrated a mode switch based on an electro-optic activated LPG formed in an LN two-mode waveguide. Their fabricated device with a z-cut LN consists of an 8-mm long LPG induced by the electro-optic effect. At a driving voltage of 35 V, it can switch between the TM_{00} and TM_{01} modes with a maximum MCE of 98.5% at a wavelength of 1544 nm and a 3-dB bandwidth of ~25 nm. Subsequently, in 2020 W. Jin *et al.* [75] further developed their proposed electro-optic activated LPG to a higher level by realizing a complete reconfigurable mode conversion for three spatial modes with three cascaded LPGs. In this work, gratings at the two ends were designed to achieve the conversion between the TM_{00} and TM_{10} modes while the grating in the middle was designed to achieve the conversion between the TM_{00} and TM_{01} modes. Their fabricated device with *z*-cut $LiNbO_3$ uses three graphene electrodes to drive the gratings and an aluminum electrode heater to achieve wavelength matching for the second grating. The use of graphene electrodes can do away with the buffer layer traditionally needed to isolate the electrodes from the waveguide, and, hence, reduce the grating driving voltage. Their typical fabricated device, which is 26-mm long, shows that the half-π voltages of the three EO activated gratings are of 48 V, 37 V, and 43 V, respectively, and the maximum MCE of the gratings at ~1545 nm is higher than 99%.

In addition, in 2018 M. R. Zhang *et al.* [76] proposed and demonstrated an LN optical waveguide ADC for the realization of an electro-optically switchable mode conversion. Their typical fabricated device for the conversion of the LP_{01} and LP_{11a} modes achieves a maximum MCE higher than 90% and the operation wavelength can be tuned over a wide range of ~240 nm by varying the driving voltage between −23 V and +20 V.

To sum up, the advantages of the ADC-based mode converters are that they are capable of achieving a quite large MCE, a quite low MCT, and a large bandwidth through flexible design and varied structure. They are easy to cascade to achieve more mode conversions simultaneously in a single chip. They are also easy to incorporate the electro-optic or thermo-optic effect to achieve reconfigurable mode converters. By contrast, although the grating-based mode converters also offer partly the above advantages, their performances are slightly inferior to those of the ADC-based mode converters, especially, in the aspect of the bandwidth and MCT.

3.3 *Mode evolution type*

Operation principle of the mode evolution converters is based on the mode field adiabatic transformation. Such an evolution requires conservation of the optical wave momentum before and after evolution which is indicated by their modal effective index matching, i.e., effective indices of the two mutually converting modes should be equal or the closest. Nowadays, to implement mode converters using the mode evolution principle, several structures, including multichannel branching waveguides [77,78], asymmetric Y-junction [79-84], stacked waveguide [85], and tapered waveguide [86,87], have been proposed. Their key performances have been summarized in Table 3 in the Appendix.

In 2003 B. T. Lee *et al.* [77] proposed and demonstrated a novel mode-order converter structured with a mode splitter, four tapered waveguides, and a mode combiner. Their designed and fabricated device with polymer materials, which can convert the TE_{00} into the TE_{30} mode

and the TE_{10} into TE_{20} mode, and vice versa, shows MCTs less than −10.2 dB for all conversion at 1550 nm. Subsequently, a five-order mode converter using a similar structure was also proposed by A. L. Y. Low *et al*. in 2004 [78]. Their well-designed device allows the conversion among the TE_{00}, TE_{10}, TE_{20}, TE_{30}, and TE_{40} modes in a cyclic manner with the MCEs larger than 93.88% and the MCTs less than −12.3 dB for all conversions at 1550 nm.

The unique mode-sorting characteristics of asymmetric Y-junctions make it an important structure for the mode conversion implementation. In 2012 N. Riesen and J. D. Love [79] extended a quantitative description of the performance of mode-conversion in bimodal Y-junctions to *N*-arm Y-junctions with *N* modes in the stem. To demonstrate their developed design criteria for optimal mode-sorting, they presented the cases of three- and four-arm asymmetric Y-junctions for the conversion among the second, third, and fourth modes in the stem into the first (fundamental) mode of different output arms, respectively. In 2013 J. B. Driscoll *et al*. [80] designed and fabricated a silicon waveguide asymmetric Y -junction mode (de)multiplexer. The device can achieve mode conversion between the fundamental and the first odd mode with a minimum MCT of -30 dB at 1580 nm, the MCT less than −9 dB over the C band, and the on-chip IL less than 1.5 dB. In 2016 J. Feng *et al*. [81] designed and fabricated a two-mode asymmetric Y-junction with polymer materials for the conversion between the LP_{01} and LP_{11a} modes. Their experimental results show that the MCT is –22.2 dB at the wavelength of 1550 nm and the 10-dB bandwidth is of ~40 nm. In 2016 W. W. Chen *et al*. [82] designed and fabricated a three-mode (de)multiplexer with SOI based on two cascaded asymmetric Y-junctions (CAYJ). Their measured results show that the MCTs for a pair of fabricated CAYJ-based three-mode (de)multiplexers are between −31.5 dB and −9.7 dB within a bandwidth from 1537 nm to 1566 nm. The measured insertion loss is less than 5.7 dB at a wavelength of 1550 nm. In 2018 T. Fujisawa *et al*. [83] proposed and fabricated with silica a novel scrambling-type mode multiplexer based on a cascaded Y-branch waveguide and an integrated mode rotator. Their proposed device is for the implementation of the LP_{01}-LP_{11a} and the LP_{01}-LP_{11b} conversions with a moderate MCE to mix these three modes. However, no experimental and theoretical MCE or MCT are presented in that work. In 2019 Y. Gao *et al*. [84] proposed a six-mode (de)multiplexer based on a 3-arm asymmetric Y-junction cascaded in each arm with a mode rotator and then a 2-arm asymmetric Y-junctions. Their designed device for the TM polarization achieves the conversions of the E_{11}-E_{21} and E_{11}-E_{31} modes with an asymmetric Y-junction directly, and the conversions of the E_{11}-E_{12}, E_{11}-E_{22}, and E_{11}-E_{32} modes with an asymmetric Y-junction combined with the aid of a mode rotator. Their simulated MCTs are less than −24 dB and the on-chip ILs are less than 0.96 dB at the operation wavelength of 1550 nm.

In 2015 T. Watanabe and Y. Kokubun [85] proposed a mode-evolutional (de)multiplexer using stacked polymer waveguides to achieve the conversion of the TE_{00}-TE_{10} and the TE_{00}-TE_{01} modes. Their fabricated device achieves the MERs from 6.5 dB to 9.7 dB for the case of LP_{10} and from 6.4 dB to 8.7 dB for the case of LP_{01} for both the TE and TM polarized modes within the C + L band.

The mode converters based on a tapered waveguide are particularly noteworthy for their unique function to convert the modes with different polarizations. In 2012 D. X. Dai *et al*. [86] investigated theoretically and experimentally the mode conversion between the TM fundamental mode and the TE higher-order modes in tapered submicron silicon ridge optical waveguides due to the mode hybridization. Their simulation results show that a very high MCE close to 100% could be achieved in both the regular lateral taper and the bi-level taper SOI rib waveguides for the conversion from the TM_0 to the TE_1 and TE_3 modes. Meanwhile, their experimental results also demonstrated the mode conversion from the TM_0 to TE_1 mode, but no MCE data were presented. Afterwards, in 2015, D. X. Dai and M. Mao [87] proposed a mode converter formed with a SOI inverse taper buried in a SiN strip waveguide again. Their designed device enables the conversion of the TE_{11}, TE_{21}, TE_{31}, TE_{41}, TM_{11}, and TM_{12} modes in a multimode SOI waveguide into the TM_{11}, TE_{11}, TE_{12}, TM_{21}, TM_{12}, and TE_{21} modes (which are like the LP_{01}, LP_{11a}, LP_{11b} modes in a few-mode fiber) in a SiN strip waveguide, with the MCEs higher than 95.6% for all desired mode conversions and negligible losses.

In general, the mode evolution converters can achieve a quite large bandwidth but with a slightly large MCT usually. In addition, it is difficult to incorporate the electro-optic or thermo-optic effect to achieve reconfigurable mode converters because a quite precise tuning for the refractive index of the involved waveguides is required.

4. Conclusions

A wide range of PLC-based mode converters has been reviewed in this paper which covers the basic principles, materials, structures, and performances of such devices. Undoubtedly, remarkable advancements have been made through the efforts of a global community of researchers and engineers. Nowadays, the ADC-based mode converters have shown excellent comprehensive performance and promising application prospects. However, to make the PLC-based mode converters to meet the requirements of the future MDM systems, there are still several key issues needed to be overcome. For the mode converters used in the MDM fiber communication system, firstly, it is still necessary to further minimize the complexity, reduce the IL and MCT, and improve efficiency of the mode conversions, especially, for the LP_{01}-LP_{11b}, LP_{01}-LP_{21a}, LP_{01}-LP_{21b}, and LP_{01}-LP_{02} mode conversions. Among these reported mode converters, only a few devices can realize the LP_{01}-LP_{21a}, LP_{01}-LP_{21b}, and LP_{01}-LP_{02} mode conversions, but they are complex and with low MCE which cannot meet the requirement for the practical applications. Secondly, it is impending to achieve simple and high-efficiency mode conversions between the fundamental mode and the fourth (including the degenerated LP_{12} and LP_{31} modes), as well as the fifth (including the LP_{03} and the degenerated LP_{22}, and LP_{41} modes) mode group so that to (de)multiplex more modes in the MDM fiber transmission system. Up to now, there are no reports on the mode conversion above. At last, it is significant to further research and develop high-performance reconfigurable or switchable mode converters able to manipulate all the first six modes due to the fact that

they are basic building blocks for the reconfigurable or switchable mode (de)multiplexer used to realize the agile MDM optical networks. As for the mode converters used in the MDM on-chip optical interconnection system, similar conclusions hold true.

Authors' statement

Research concept and design, writing the article, collecting and assembly of data, Areez Khalil Memon; Research concept and design, critical revision of the article, final approval of article, Kai Xin Chen.

Acknowledgements

This work was supported in part by the National Natural Science Foundation of China (62075027), in part by the Key R & D Program of Sichuan Province (2020YFSY0003), and in part by the Fundamental Research Funds for the Central Universities (ZYGX2019J050).

Appendix

Table 1
Key performances of the mode converters based on the mode reconstitution principle.

Device structure	Device characteristics					
	Converting Modes	MCE, MCT, MER (dB)	IL On-chip IL MCL (dB)	Operation wavelength and Bandwidth (3 dB, nm)	Material and Research type	Year and Ref.
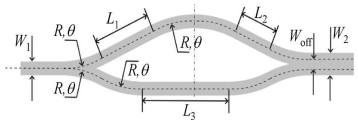	The zero- and first-order modes	MCE = 94% (Theoretical)	MCL = 0.4	1550 nm NR	InP/BCB Experimental work	2006 [22]
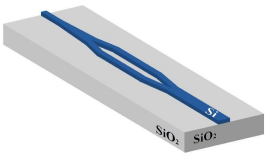	The fundamental and the higher odd modes	NR	NR	1550 nm NR	SOI Theoretical work	2015 [23]
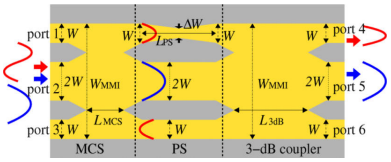	The fundamental and first-order modes, (TM)	MCE = ~90%	NR	1530–1565 nm	SOI Theoretical work	2012 [24]
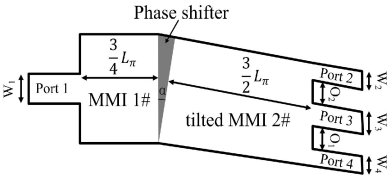	The fundamental and first-order modes	MCT < –28	On-chip IL: < 1	1530–1565 nm NR	Si/SiO_2 Theoretical work	2015 [25]
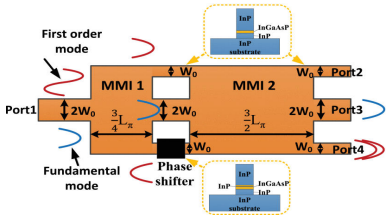	TE_0-TE_1	MCE = ~100% (Theoretical) MCT < –18.4 (Theoretical)	On-chip IL: < 1.2 (Theoretical)	1530–1565 nm (Theoretical)	InP/InGaAsP Experimental work	2016 [26]
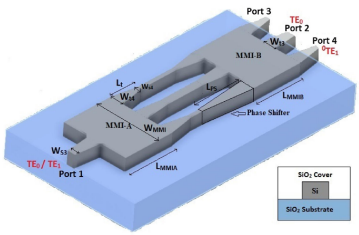	TE_0-TE_1	MCT < –20	On-chip IL: IL < 1.8	1520–1580 nm	SOI Experimental work	2020 [27]

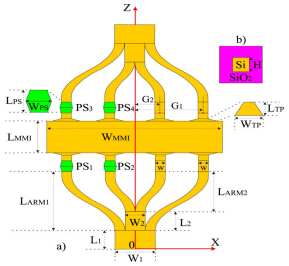	TE_i-TE_j i, j = 0, 1, 2, 3	MCE > 98% MCT < –30	On-chip IL: < 0.8	1530–1565 nm	SOI Theoretical work	2019 [28]
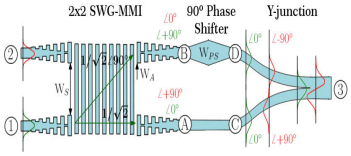	TE_0-TE_1	MCT < –20	On-chip IL: < 0.84	1400–1700 nm	SOI Theoretical work	2018 [29]
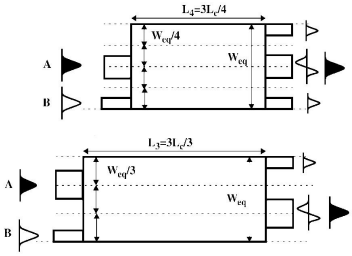	The fundamental and the transversal first-order mode	NR	MCL < 0.3	1550 nm NR	InP/InGaAsP Experimental work	1998 [30]
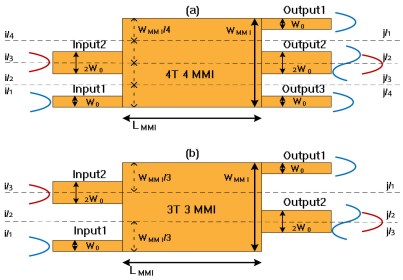	TE_0-TE_1	NR	Relative IL < 3.9 (50% type) < 1 (66% type)	1280–1320 nm	InP/InGaAsP Experimental work	2016 [31]
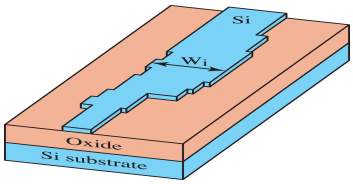	The fundamental and the first-higher order high mode	MCE = 94.2%	NR	1550 nm NR	SOI Theoretical work	2006 [32]
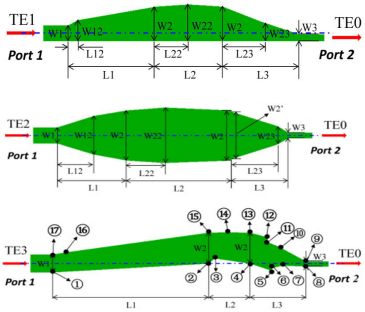	TE_1-TE_0 TE_2-TE_0 TE_3-TE_0 TE_2-TE_1 TE_3-TE_1 TE_3-TE_2	98.6% 98.8% 97.5% 97.3% 96.2% 96.5%	MCL: 0.061 0.052 0.11 NR NR NR	1520–1580 nm	SOI Theoretical work	2015 [33]
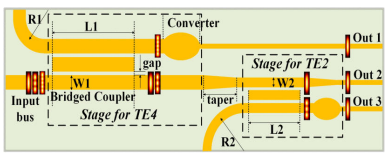	TE_{00}-TE_{02} TE_{00}-TE_{04}	MCT < –19 MCT < –16	NR	1525–1585 nm	SOI Experimental work	2018 [34]

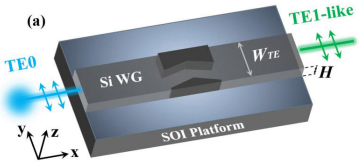	TE_0-TE_1 TM_0-TM_1	MCE > 97%	NR	1500–1600 nm	SOI/HRIM Theoretical work	2018 [35]
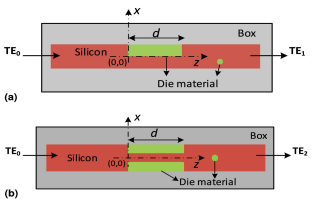	TE_0-TE_1 TE_0-TE_2	MCT: < –13.4055 < –12.6240	On-chip IL: = 2.0875 = 1.3745	1550 nm NR	SOI Experimental work	2019 [36]
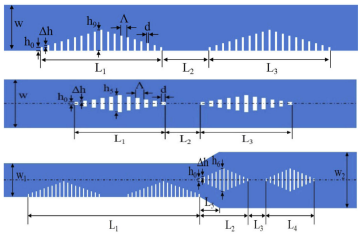	TE_0-TE_1 TE_0-TE_2 TE_0-TE_3	MCE: > 94.4% > 95.7% > 83.7% MCT: < –15.33 < –17.36 < –15.65	NR	1500–1600 nm	SOI Theoretical work	2019 [37]
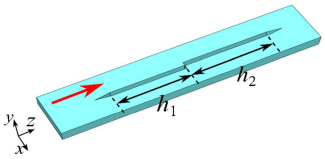	TE_0 like-TE_1 like	MCE: > 95%	NR	1420–1620 nm	SOI Theoretical work	2017 [38]
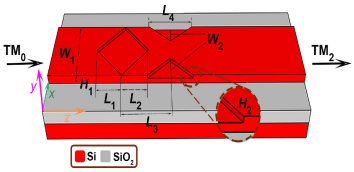	TM_0-TM_2	MCE > 94% MCT < –15	On-chip IL: < 0.5	1458–1586 nm	SOI_2 Theoretical work	2019 [39]
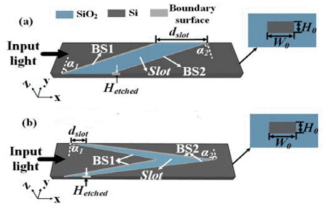	TE_0-TE_1 TE_0-TE_2	MCE: 99.7% 99.4% MCT: < –26.4 < –27.3	NR	1500–1600 nm	SOI Theoretical work	2019 [40]
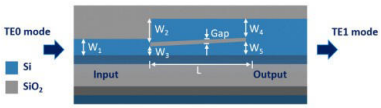	TE_0-TE_1	MCT: < –6.3	On-chip IL < 1.2	1520–1570 nm	SOI Experimental work	2020 [41]
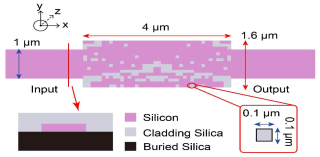	TE_0-TE_1 TM_0-TM_1	MCT: < –13.7 < –11.8	On-chip IL: 1.0-2.3 (TE) 0.9-1.4 (TM)	1525–1565 nm NR	Si/SiO_2 Experimental work	2019 [42]
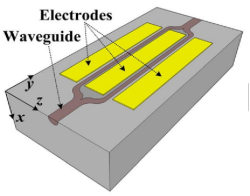	TE_{11}-TE_{21}	MER: ~35	IL: ~8	1552 nm ~12 (20 dB)	LN Experimental work	2016 [43]

Table 2
Key performances of the mode converters based on the mode coupling principle.

Device structure	Device characteristics					
	Converting Modes	MCE, MCT, MER (dB)	IL On-chip IL MCL (dB)	Operation wavelength and Bandwidth (3 dB, nm)	Material and Research type	Year and Ref.
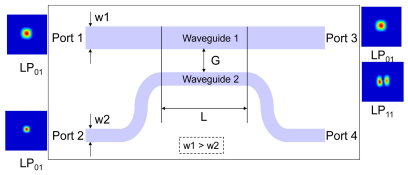	LP_{01}-LP_{11}	MER > 15	IL: 1.3	C-band	Silica Experimental work	2012 [44]
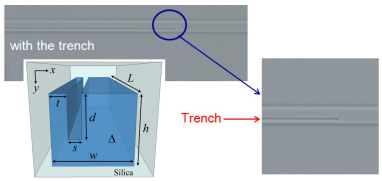	LP_{11a}-LP_{11b}	MCE > 90%	NR	1450–1650 nm	Silica Experimental work	2014 [45]
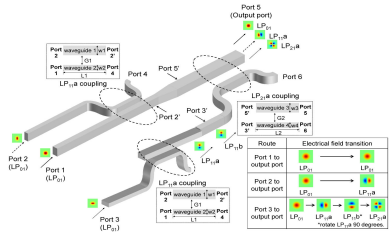	LP_{01}-LP_{11a} LP_{01}-LP_{11a}-LP_{11b}-LP_{21a}	MER > 13	IL < 3.5	C-band	Silica Experimental work	2014 [46]
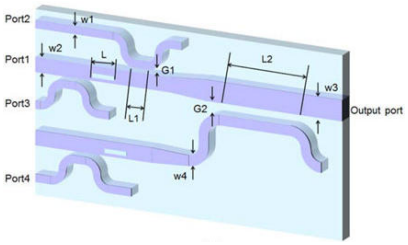	LP_{01}-LP_{11a} LP_{01}-LP_{11a} - LP_{11b} LP_{01}-LP_{11a}-LP_{11b}-LP_{21a}	MER > 12	IL < 3.5	1530–1560 nm	Silica Experimental work	2015 [47]
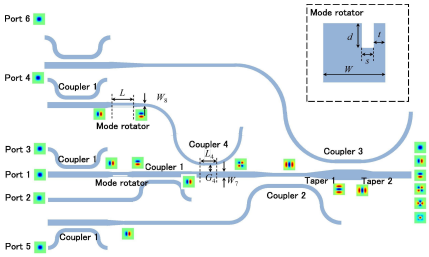	LP_{01}-LP_{11a} LP_{01}-LP_{11a}-LP_{11b} LP_{01}-LP_{11a}-LP_{11b}-LP_{21a} LP_{01}-LP_{11a}-LP_{31a}-LP_{31b}-LP_{21b} LP_{01}-LP_{11a}-LP_{31a}-LP_{02}	NR	NR	1530–1565 nm	Silica Experimental work	2016 [48]
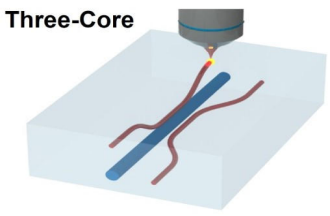	LP_{01}-LP_{11a} LP_{01}-LP_{11b}	MCE: 53% to 68% 80% to 99% MER: 25 to 32 35 to 37	IL: ~1	1500–1580 nm	Boro-aluminosilicate Experimental work	2014 [49]

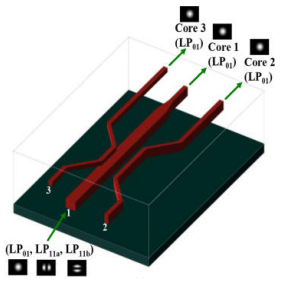	LP_{01}-LP_{11a} LP_{01}-LP_{11b}	MCE: 91% to 99% MCT: –23.2 to –14.1	IL: ~10	1530–1570 nm	Epocore/ Epoclad Experimental work	2015 [50]
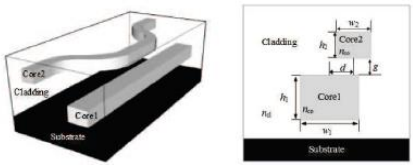	LP_{01}-LP_{21a}	MCE: 98.7%	NR	1550 nm 40 (10 dB)	Epocore/ Epoclad Experimental work	2016 [51]
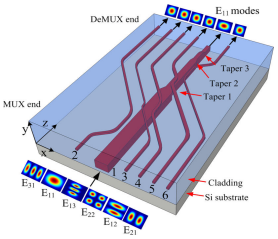	E_{11}-E_{21} E_{11}-E_{12} E_{11}-E_{22} E_{11}-E_{31} E_{11}-E_{13}	MCE: 62% to 90% MCT: –28.2 to –11.6	IL: 8.9-11.5	1530–1565 nm	Epocore/ Epoclad Experimental work	2016 [52]
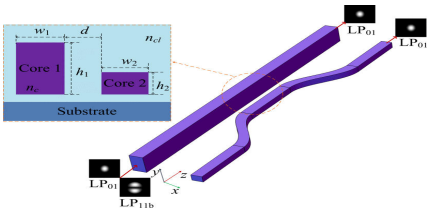	LP_{01}-LP_{11b}	MCE > 95%	IL: 12.8	1530–1560 nm	Epocore/ Epoclad Experimental work	2017 [53]
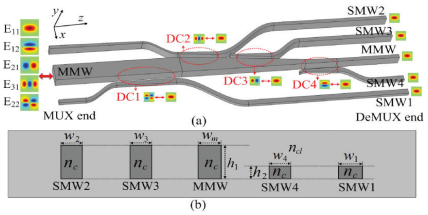	E_{11}-E_{21} E_{11}-E_{12} E_{11}-E_{22} E_{11}-E_{31}	MCE > 94.5%	IL: 10.6-19.1	C+L band	Epocore/ Epoclad Experimental work	2019 [54]
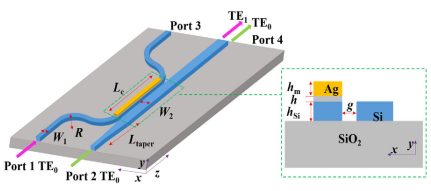	TE_0-TE_1	MCE = 99.2% MCT < –17	NR	1500–1600 nm	SOI Ag plasmonic Experimental work	2014 [55]
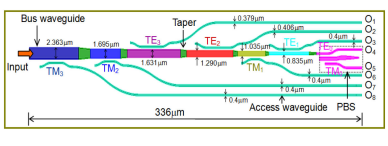	TE_0-TE_1 TE_0-TE_2 TE_0-TE_3 TM_0-TM_1 TM_0-TM_2 TM_0-TM_3	MCT: –11 to –20	NR	1520–1610 nm	SOI Experimental work	2014 [56]

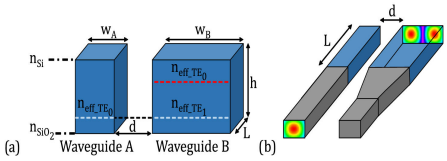	TE_0-TE_1	MCE: 84% to 90%	NR	1550 nm 20	SOI Experimental work	2017 [57]
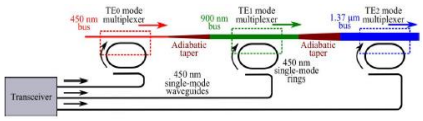	TE_0-TE_1 TE_0-TE_2	MCT < –20	NR	1547.4 nm	SOI Experimental work	2013 [58]
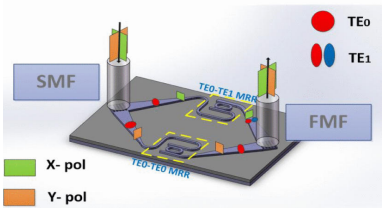	LP_{01}-LP_{11}	MCT = –20	NR	1550.17 nm FSR = ~6.2 nm	SOI Experimental work	2015 [59]
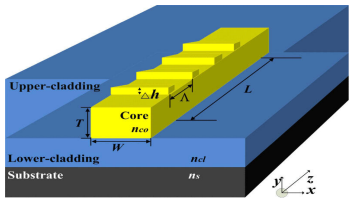	LP_{01}-LP_{11b}	MCE = ~99% at 1536 nm	NR	1536 nm 4	Epocore/ Epoclad Experimental work	2015 [60]
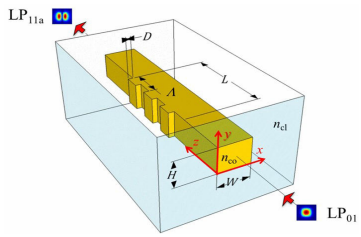	LP_{01}-LP_{11a}	MCE > 99% at 1600 nm	NR	1600 nm 20	Epocore/ Epoclad Experimental work	2015 [61]
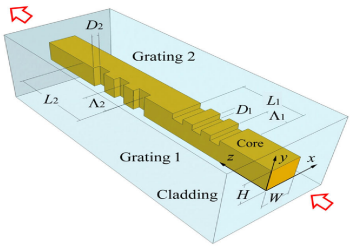	LP_{01}-LP_{11a}-LP_{11b}-LP_{01} LP_{01}-LP_{21a}	MCE = 94% at 1540 nm MCE = 90% at 1550 nm	IL: ~ 7.9	1540 nm 1550 nm	Epocore/ Epoclad Experimental work	2016 [62]
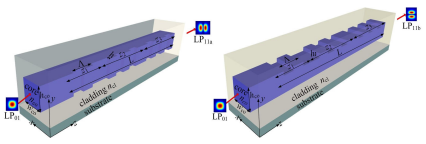	LP_{01}-LP_{11a} LP_{01}-LP_{11b}	MCE > 99% MCE > 90 MCE > 99% MCE > 90%	NR	(10 dB) 120 (20 dB) 150 (10 dB) 180 (20 dB) 300	Epocore/ Epoclad Experimental work	2017 [63]
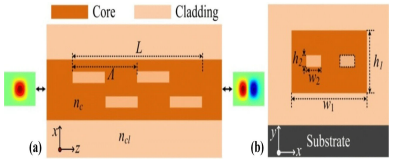	E_{11}-E_{12}	MCE > 98.2%	IL: ~6.4	C+L band	Epocore/ Epoclad Experimental work	2019 [64]

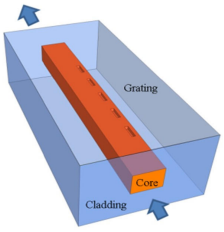	E_{11}-E_{12} E_{11}-E_{22} E_{12}-E_{21}	MCE > 98% at 1545nm MCE > 95% at 1575nm MCE > 94% at 1550nm	NR	1550 nm 1575 nm 1550 nm	Epocore/ Epoclad Experimental work	2018 [65]
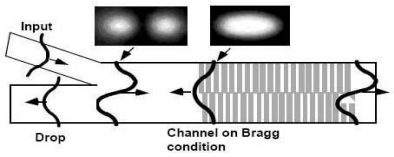	Even-Odd modes (E_{11}-E_{21})	MCE > 99%	NR	1551.35 (TE) 1551.6 (TM)	SiO_2 Experimental work	2005 [66]
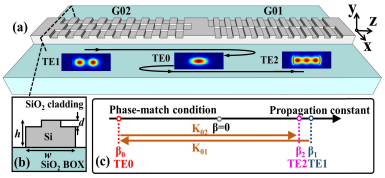	TE_1-TE_0-TE_2	MCT = ~–7	NR	1525 nm 9	SOI Experimental work	2019 [67]
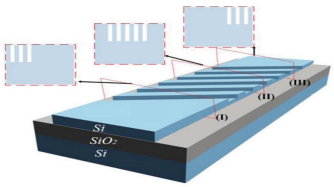	TE_0-TE_1 TE_0-TE_2	MCT < –10	MCL: < 1.0 < 0.5	1542–1563 nm 1545–1565 nm	SOI Experimental work	2019 [68]
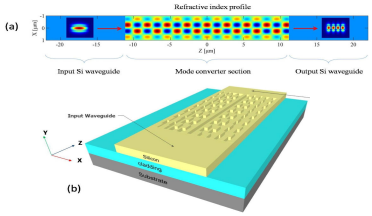	TM_0-TM_1 TM_0-TM_2 TM_0-TM_3	MCE: > 97% > 97% > 96% MCT: < –27.9 < –45.1 < –23.9	NR	1550 nm	SOI Theoretical work	2014 [69]
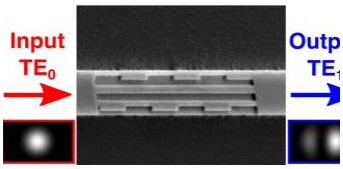	TE_0-TE_1	Mode purity: 95%	NR	1550 nm	SOI Experimental work	2016 [70]
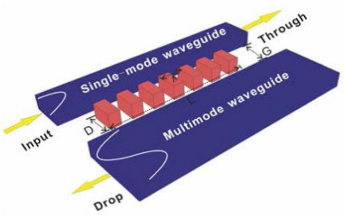	Fundamental mode to the 1st, 2nd, 3rd modes (TE_0-TE_1 TE_0-TE_2 TE_0-TE_3)	MCT: –22.6 –26.8 –30.3	On-chip IL: 0.2, 0.34 0.21	1550 nm 4 7.6 12.8	SOI Theoretical work	2013 [71]
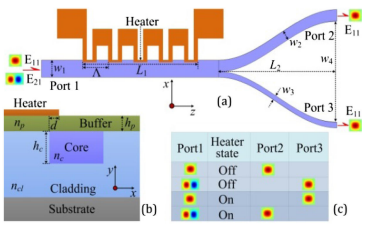	Switchable E_{11}-E_{21}	Mode Selectivity > 12	IL: ~12	C+L band	Epocore /Epoclad Experimental work	2018 [72]

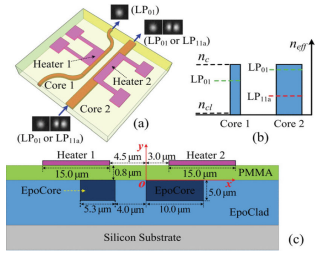	Switchable LP$_{01}$-LP$_{11a}$	MER > 10	11	C+L band	Epocore /Epoclad Experimental work	2018 [73]
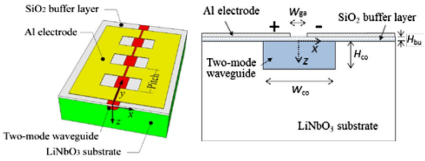	Switchable TM$_{00}$-TM$_{01}$	MCE = 98.5 at 1544 nm	NR	1544 nm 25	LN Experimental work	2015 [74]
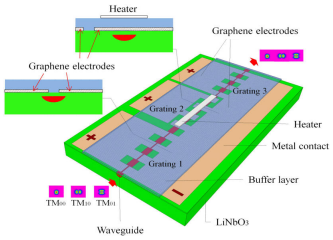	Switchable TM$_{00}$-TM$_{01}$ TM$_{00}$-TM$_{10}$	MCE > 99% at 1545 nm	NR	1545 nm	LN Experimental work	2020 [75]
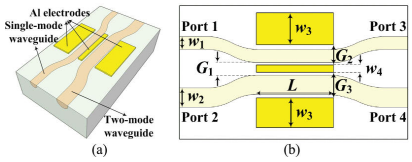	Switchable LP$_{01}$-LP$_{11a}$	MCE > 90%	< 5dB	~240 nm with a driving voltage in the range from −23 V to +20 V.	LN Experimental work	2018 [76]

Table 3
Key performances of the mode converters based on the mode evolution principle.

Device structure	Device characteristics					
	Converting Modes	MCE, MCT, MER (dB)	IL On-chip IL MCL (dB)	Operation wavelength and Bandwidth (3 dB, nm)	Material and Research type	Year and Ref.
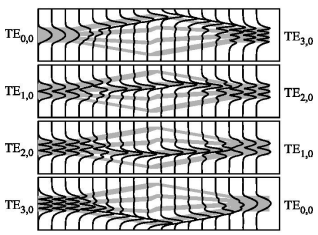	TE$_{00}$-TE$_{30}$ TE$_{10}$-TE$_{20}$	MCT < 10.2	NR	1550 nm NR	BCB/UV-15 Experimental work	2003 [77]
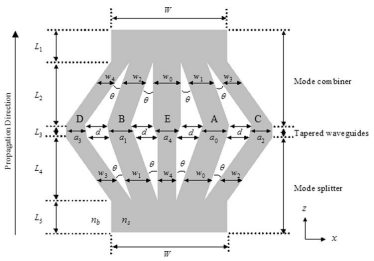	TE$_{00}$-TE$_{10}$ TE$_{10}$-TE$_{20}$ TE$_{20}$-TE$_{30}$ TE$_{30}$-TE$_{40}$ TE$_{40}$-TE$_{00}$	MCE > 93.88% MCT < –12.3	NR	1550 nm NR	NR Theoretical work	2004 [78]

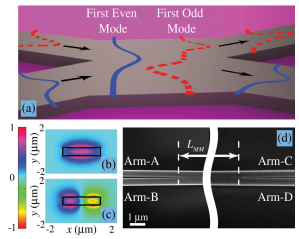	Fundamental and first odd mode	MCT: –30 (1580 nm) < –9 (C band)	On-chip IL: < 1.5	1580 nm C band	SOI Experimental work	2013 [80]
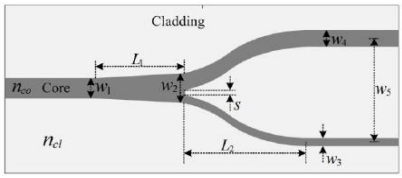	LP_{01}-LP_{11a}	MCT = –22.2	IL: ~13.2	1560 nm (10 dB) 40	Epoclad/ Epocore Experimental work	2016 [81]
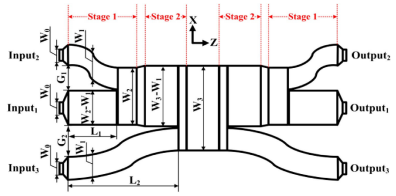	TE_0-TE_1 TE_0-TE_2 TE_0-TE_3	MCT: –31.5 to –9.7	IL: 5.7 dB at 1550 nm	1537–1566 nm	SOI Experimental work	2016 [82]
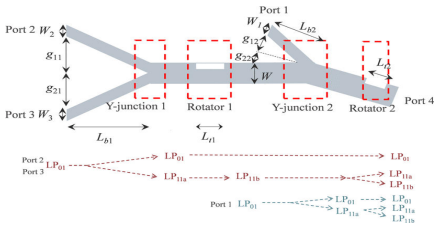	LP_{01}-LP_{11a} LP_{01}-LP_{11b}	NR	NR	1550 nm NR	Silica Experimental work	2018 [83]
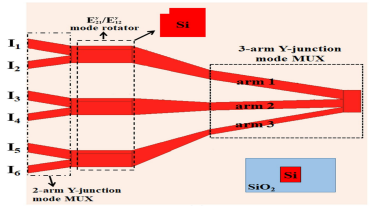	E_{11}-E_{21} E_{11}-E_{31} E_{11}-E_{21}-E_{12} E_{11}-E_{21}-E_{12}-E_{22} E_{11}-E_{21}-E_{12}-E_{32}	MCT < –24	On-chip IL: < 0.96	1525–1565 nm	SOI Theoretical work	2019 [84]
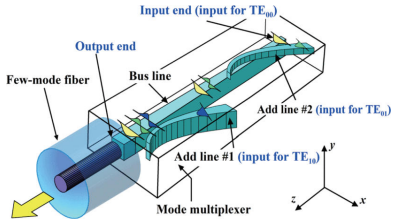	TE_{00}-TE_{10} TE_{00}-TE_{01}	MER: 6.5 to 9.7 6.4 to 8.7	IL: 9.0 to 11.6	C+L band	PMMA/Epoxy resin Experimental work	2015 [85]
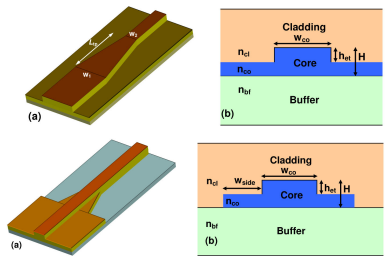	Simulation: TM_0-TE_1 TM_0-TE_3 Experiment: TM_0-TE_1	Simulation: MCE = ~100% Experiment: NR	NR	1550 nm NR	SOI Experimental work	2012 [86]
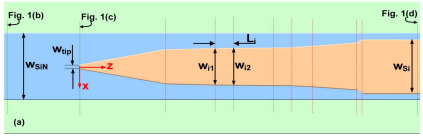	SOI-SiN TE_{11}-TE_{11} TE_{21}-TM_{11} TE_{31}-TE_{12} TE_{41}-TM_{12} TM_{21}-TE_{21} TE_{11}-TM_{21}	MCE > 95.6%	NR	1550 nm NR	SOI SiN Theoretical work	2015 [87]

References

[1] Essiambre, R. -J., Kramer, G., Winzer, P. J., Foschini, G. J. & Goebel, B. Capacity limits of optical fiber networks. *J. Lightwave Technol.* **28**, 662–701 (2010). https://doi.org/10.1109/JLT.2009.2039464

[2] CISCO: Cisco Visual Netwroking Index: Forecast and Trends, 2017–2022 *White Paper* [Online]. Available at: https://www.cisco.com/c/en/us/solutions/collateral/service-provider/visual-networking-index-vni/white-paper-c11-741490.html. (Accessed: 19th September 2020)

[3] Agrell, E. *et al*. Roadmap of optical communications. *J. Opt.* **18**, 063002 (2016). http://dx.doi.org/10.1088/2040-8978/18/6/063002

[4] Tkach, R. W. Scaling optical communications for the next decade and beyond. *Bell Labs Tech. J.* **14**, 3–10 (2010). https://doi.org/10.1002/bltj.20400

[5] Yu, J. & Zhang, J. Recent progress on high-speed optical transmission. *Digit. Commun. Netw.* **2**, 65–76 (2016). http://dx.doi.org/10.1016/j.dcan.2016.03.002

[6] Abbas, H. S. & Gregory, M. A. The next generation of passive optical networks: A review. *J. Netw. Comput. Appl.* **67**, 53–74 (2016). http://dx.doi.org/10.1016/j.jnca.2016.02.015

[7] Sillard, P. Next-generation fibers for space-division-multiplexed transmissions. *J. Lightwave Technol.* **33**, 1092–1099 (2015). https://doi.org/10.1109/JLT.2014.2371134

[8] Richardson, D., Fini, J. & Nelson, L. E. Space-division multiplexing in optical fibres. *Nat. Photonics* **7**, 354–362 (2013). https://doi.org/10.1038/nphoton.2013.94

[9] Klaus, W. *et al*. Advanced space division multiplexing technologies for optical networks. *J. Opt. Commun. Netw.* **9**, C1–C11 (2017). https://doi.org/10.1364/JOCN.9.0000C1

[10] Nakazawa, M. Exabit optical communication explored using 3M scheme. *Jap. J. Appl. Phys.* **53**, , 08MA01 (2014). http://dx.doi.org/10.7567/JJAP.53.08MA01

[11] Winzer, P. J. Optical networking beyond WDM. *IEEE Photonics J.* **4**, 647–651 (2012). https://doi.org/10.1109/JPHOT.2012.2189379

[12] Chiang, K. S. Polymer optical waveguide devices for mode-division-multiplexing applications. *Proc. SPIE 10242, Integrated Optics: Physics and Simulations III*, 102420R (2017). https://doi.org/10.1117/12.2265275

[13] Sabitu, R., Khan, N. & Malekmohammadi, A. Recent progress in optical devices for mode division multiplex transmission system. *Opto-Electron. Review* **27**, 252–267 (2019). https://doi.org/10.1016/j.opelre.2019.07.001

[14] Ryf, R., Fontaine, N. K., Guan, B., Huang, B. & Tkach, R. W. 305-km combined wavelength and mode-multiplexed transmission over conventional graded-index multimode fibre. in *The European Conference on Optical Communication (ECOC)*, 1–3 (2014).

[15] Hayashi, T. *et al*. Six-mode 19-core fiber with 114 spatial modes for weakly-coupled mode-division-multiplexed transmission. *J. Lightwave Technol.* **35**, 748–754 (2017). https://doi.org/10.1109/JLT.2016.2617894

[16] Soma, D. *et al*. 10.16-Peta-B/s dense SDM/WDM transmission over 6-mode 19-core fiber across the C+ L band. *J. Lightwave Technol.* **36**, 1362–1368 (2018). https://doi.org/10.1364/JLT.36.001362

[17] Van Uden, R. *et al*. Ultra-high-density spatial division multiplexing with a few-mode multicore fibre. *Nat. Photon.* **8**, 865–870 (2014). https://doi.org/10.1038/nphoton.2014.243

[18] Dai, D. X. & Bowers, J. E. Silicon-based on-chip multiplexing technologies and devices for Peta-bit optical interconnects. *Nanophotonics* **3**, 283–311 (2014). https://doi.org/10.1515/nanoph-2013-0021

[19] Luo, L. -W. *et al*. WDM-compatible mode-division multiplexing on a silicon chip. *Nat. Commun.* **5**, 1–7 (2014). https://doi.org/10.1038/ncomms4069

[20] Hsu, Y. *et al*. 2.6 Tbit/s on-chip optical interconnect supporting mode-division-multiplexing and PAM-4 signal. *IEEE Photonics Technol. Lett.* **30**, 1052–1055 (2018). https://doi.org/10.1109/LPT.2018.2829508

[21] Zhang, W., Ghorbani, H., Shao, T. & Yao, J. On-Chip 4×10 GBaud/s Mode-Division Multiplexed PAM-4 Signal Transmission. *IEEE J. Sel. Top. Quantum Electron.* **26**, 1–8 (2020). https://doi.org/10.1109/JSTQE.2020.2964388

[22] Huang, Y., Xu, G. & Ho, S. -T. An ultracompact optical mode order converter. *IEEE Photonics Technol. Lett.* **18**, 2281–2283 (2006). https://doi.org/10.1109/LPT.2006.884886

[23] Oner, B., Üstün, K., Kurt, H., Okyay, A. K. & Turhan-Sayan, G. Large bandwidth mode order converter by differential waveguides. *Opt. Express* **23**, 3186–3195 (2015). https://doi.org/10.1364/OE.23.003186

[24] Uematsu, T., Ishizaka, Y., Kawaguchi, Y., Saitoh, K. & Koshiba, M. Design of a compact two-mode multi/demultiplexer consisting of multimode interference waveguides and a wavelength-insensitive phase shifter for mode-division multiplexing transmission. *J. Lightwave Technol.* **30**, 2421–2426 (2012). https://doi.org/10.1109/JLT.2012.2199961

[25] Han, L., Liang, S., Zhu, H., Qiao, L., Xu, J. & Wang, W. Two-mode de/multiplexer based on multimode interference couplers with a tilted joint as phase shifter. *Opt. Lett.* **40**, 518-521 (2015). http://dx.doi.org/10.1364/OL.40.000518

[26] Guo, F. *et al*. An MMI-based mode (DE) MUX by varying the waveguide thickness of the phase shifter. *IEEE Photonics Technol. Lett.* **28**, 2443–2446 (2016). https://doi.org/10.1109/LPT.2016.2599934

[27] Chack, D., Hassan, S. & Qasim, M. Broadband and low crosstalk silicon on-chip mode converter and demultiplexer for mode division multiplexing. *Appl. Opt.* **59**, 3652–3659 (2020). https://doi.org/10.1364/AO.390085

[28] Linh, H. D. T., Dung, T. C., Tanizawa, K., Thang, D. D. & Hung, N. T. Arbitrary $TE_0/TE_1/TE_2/TE_3$ Mode Converter Using 1× 4 Y-Junction and 4× 4 MMI Couplers. *IEEE J. Sel. Top. Quantum Electron.* **26**, 1–8 (2019). https://doi.org/10.1109/JSTQE.2019.2937169

[29] González-Andrade, D. *et al*. Ultra-broadband mode converter and multiplexer based on sub-wavelength structures. *IEEE Photonics J.* **10**, 1–10 (2018). https://doi.org/10.1109/JPHOT.2018.2819364

[30] Leuthold, J., Eckner, J., Gamper, E., Besse, P. A. & Melchior, H. Multimode interference couplers for the conversion and combining of Zero- and First-Order modes. *J. Lightwave Technol.* **16**, 1228–1239 (1998). https://doi.org/10.1109/50.701401

[31] Guo, F. *et al*.Two-mode converters at 1.3 μm based on multimode interference couplers on InP substrates. *Chin. Phys. Lett.* **33**, 024203 (2016). http://dx.doi.org/10.1088/0256-307X/33/2/024203

[32] Chen, H. -T. & Webb, K. J. Silicon-on-insulator irregular waveguide mode converters. *Opt. Lett.* **31**, 2145–2147 (2006). https://doi.org/10.1364/OL.31.002145

[33] Chen, D. *et al*. Low-loss and fabrication tolerant silicon mode-order converters based on novel compact tapers. *Opt. Express* **23**, 11152–11159 (2015). https://doi.org/10.1364/OE.23.011152

[34] Chen, Z. Y. Bridged coupler and oval mode converter based silicon mode division (de)multiplexer and Terabit WDM-MDM system demonstration. *J. Lightwave Technol.* **36**, 2757–2766 (2018). https://dx.doi.org/10.1109/JLT.2018.2818793

[35] Zhu, D. *et al*. Design of compact TE-polarized mode-order converter in silicon waveguide with high refractive index material. *IEEE Photonics J.* **10**, 1–7 (2018). https://doi.org/10.1109/JPHOT.2018.2883209

[36] Abu-Elmaaty, B. E., Sayed, M. S., Pokharel, R. K. & Shalaby, H. M. General silicon-on-insulator higher-order mode converter based on substrip dielectric waveguides. *Appl. Opt.* **58**, 1763–1771 (2019). https://doi.org/10.1364/AO.58.001763

[37] Cheng, Z. *et al*. Sub-wavelength grating assisted mode order converter on the SOI substrate. *Opt. Express* **27**, 34434–34441 (2019). https://doi.org/10.1364/OE.27.034434

[38] Ye, W., Yuan, X., Gao, Y. & Liu, J. Design of broadband silicon-waveguide mode-order converter and polarization rotator with small footprints. *Opt. Express* **25**, 33176–33183 (2017). https://doi.org/10.1364/OE.25.033176

[39] Liu, L. *et al*. Design of a compact silicon-based TM-polarized mode-order converter based on shallowly etched structures. *Appl. Opt.* **58**, 9075–9081 (2019). https://doi.org/10.1364/AO.58.009075

[40] Hao, L. *et al*. Efficient TE-polarized mode-order converter based on high-index-contrast polygonal slot in a silicon-on-insulator waveguide. *IEEE Photonics J.* **11**, 1–10 (2019). https://doi.org/10.1109/JPHOT.2019.2907640

[41] Zhao, Y. *et al*. Ultra-compact silicon mode-order converters based on dielectric slots. *Opt. Lett.* **45**, 3797–3800 (2020). https://doi.org/10.1364/OL.391748

[42] Jia, H. *et al*. Ultra-compact dual-polarization silicon mode-order converter. *Opt. Lett.* **44**, 4179–4182 (2019). https://doi.org/10.1364/OL.44.004179

[43] Zhang, M. R., Chen, K. X., Jin, W. & Chiang, K. S. Electro-optic mode switch based on lithium-niobate Mach–Zehnder interferometer. *Appl. Opt.* **55**, 4418–4422 (2016). https://doi.org/10.1364/AO.55.004418

[44] Hanzawa, N. *et al*. Two-mode PLC-based mode multi/demultiplexer for mode and wavelength division multiplexed transmission. *Opt. Express* **21**, 25752–25760 (2013). https://doi.org/10.1364/OE.21.025752

[45] Saitoh, K. *et al*. PLC-based LP_{11} mode rotator for mode-division multiplexing transmission. *Opt. Express* **22**, 19117–19130 (2014). https://doi.org/10.1364/OE.22.019117

[46] Hanzawa, N. *et al*. Mode multi/demultiplexing with parallel waveguide for mode division multiplexed transmission. *Opt. Express* **22**, 29321–29329 (2014). https://doi.org/10.1364/OE.22.029321

[47] Hanzawa, N. *et al*. PLC-based four-mode multi/demultiplexer with LP_{11} mode rotator on one chip. *J. Lightwave Technol.* **33**, 1161–1165 (2015). https://doi.org/10.1109/JLT.2014.2378281

[48] Saitoh, K. *et al*. PLC-based mode multi/demultiplexers for mode division multiplexing. *Opt. Fiber Technol.* **35**, 80–92 (2017). https://doi.org/10.1016/j.yofte.2016.08.002

[49] Riesen, N., Gross, S., Love, J. D. & Withford, M. J. Femtosecond direct-written integrated mode couplers. *Opt. Express* **22**, 29855–29861 (2014). https://doi.org/10.1364/OE.22.029855

[50] Dong, J. L., Chiang, K. S. & Jin, W. Compact three-dimensional polymer waveguide mode multiplexer. *J. Lightwave Technol.* **33**, 4580–4588 (2015). https://doi.org/10.1109/JLT.2015.2478961

[51] Wei, F. K., Chen, K. X. & Chiang, K. S. Mode conversion with vertical polymer-waveguide directional coupler. in *Asia Communication and Photonics Conf*erence, AF1G.3 (2016). https://doi.org/10.1364/ACPC.2016.AF1G.3

[52] Huang, Q. D., Wu, Y. F., Jin, W. & Chiang, K. S. Mode multiplexer with cascaded vertical asymmetric waveguide directional couplers. *J. Lightwave Technol.* **36**, 2903–2911 (2018). https://dx.doi.org/10.1109/JLT.2018.2829143

[53] Zhao, W. K., Chen, K. X., Wu, J. Y. & Chiang, K. S. Horizontal directional coupler formed with waveguides of different heights for mode-division multiplexing. *IEEE Photonics J.* **9**, 1–9 (2017). https://doi.org/10.1109/JPHOT.2017.2731046

[54] Zhao, W. K., Chen, K. X. & Wu, J. Y. Broadband mode multiplexer formed with non-planar tapered directional couplers. *IEEE Photonics Technol. Lett.* **31**, 169–172 (2018). https://doi.org/10.1109/LPT.2018.2887352

[55] Yin, M., Deng, Q., Li, Y., Wang, X. & Li, H. Compact and broadband mode multiplexer and demultiplexer based on asymmetric plasmonic–dielectric coupling. *Appl. Opt.* **53**, 6175–6180 (2014). https://doi.org/10.1364/AO.53.006175

[56] Wang, J., Chen, P., Chen, S., Shi, Y. & Dai, D. X. Improved 8-channel silicon mode demultiplexer with grating polarizers. *Opt. Express* **22**, 12799–12807 (2014). https://doi.org/10.1364/OE.22.012799

[57] Garcia-Rodriguez, D., Corral, J. L. Griol, A. & Llorente, R. Dimensional variation tolerant mode converter/multiplexer fabricated in SOI technology for two-mode transmission at 1550 nm. *Opt. Lett.* **42**, 1221–1224 (2017). https://doi.org/10.1364/OL.42.001221

[58] Luo, L. -W., Gabrielli, L. H. & Lipson, M. On-chip mode-division multiplexer. in *Conference on Lasers and Electro-Optics (CLEO 2013)* CTh1C.6. (2013). https://doi.org/10.1364/CLEO_SI.2013.CTh1C.6

[59] Yu, Y., Ye, M. & Fu, S. On-chip polarization controlled mode converter with capability of WDM operation. *IEEE Photonics Technol. Lett.* **27**, 1957–1960 (2015). https://doi.org/10.1109/LPT.2015.2448076

[60] Yang, Y., Chen, K. X., Jin, W. & Chiang, K. S. Widely wavelength-tunable mode converter based on polymer waveguide grating. *IEEE Photonics Technol. Lett.* **27**, 1985–1988 (2015). https://doi.org/10.1109/LPT.2015.2448793

[61] Jin, W. & Chiang, K. S. Mode converter with sidewall-corrugated polymer waveguide grating. in *Opto-Electronics Communication Conference (OECC2015)*, 1–3 (2015). https://doi.org/10.1109/OECC.2015.7340081

[62] Jin, W. & Chiang, K. S. Mode converters based on cascaded long-period waveguide gratings. *Opt. Lett.* **41**, 3130–3133 (2016). https://doi.org/10.1364/OL.41.003130

[63] Wang, W., Wu, J. Y., Chen, K. X., Jin, W. & Chiang, K. S. Ultra-broadband mode converters based on length-apodized long-period waveguide gratings. *Opt. Express* **25**, 14341–14350 (2017). https://doi.org/10.1364/OE.25.014341

[64] Zhao, W. K., Chen, K. X. & Wu, J. Y. Ultra-short embedded long-period waveguide grating for broadband mode conversion. *App. Phys. B* **125**, 177 (2019). https://doi.org/10.1007/s00340-019-7290-0

[65] Jin, W. & Chiang, K. S. Three-dimensional long-period waveguide gratings for mode-division-multiplexing applications. *Opt. Express* **26**, 15289–15299 (2018). https://doi.org/10.1364/OE.26.015289

[66] Castro, J. M. *et al*. Demonstration of mode conversion using anti-symmetric waveguide Bragg gratings. *Opt. Express* **13**, 4180–4184 (2005). https://doi.org/10.1364/OPEX.13.004180

[67] Xiao, R. *et al*. On-chip mode converter based on two cascaded Bragg gratings. *Opt. Express* **27**, 1941–1957 (2019). https://doi.org/10.1364/OE.27.001941

[68] Wang, H. *et al*. Compact silicon waveguide mode converter employing dielectric metasurface structure. *Adv. Opt. Mater.* **7**, 1801191 (2019). https://doi.org/10.1002/adom.201801191

[69] Ohana, D. & Levy, U. Mode conversion based on dielectric metamaterial in silicon. *Opt. Express* **22**, 27617–27631 (2014). https://doi.org/10.1364/OE.22.027617

[70] Ohana, D., Desiatov, B., Mazurski, N. & Levy, U. Dielectric metasurface as a platform for spatial mode conversion in nanoscale waveguides. *Nano Lett.* **16**, 7956–7961 (2016). https://doi.org/10.1021/acs.nanolett.6b04264

[71] Qiu, H. *et al*. Silicon mode multi/demultiplexer based on multimode grating-assisted couplers. *Opt. Express* **21**, 17904–17911 (2013). https://doi.org/10.1364/OE.21.017904

[72] Zhao, W. K., Feng, J., Chen, K. X. & Chiang, K. S. Reconfigurable broadband mode (de) multiplexer based on an integrated thermally induced long-period grating and asymmetric Y-junction. *Opt. Lett.* **43**, 2082–2085 (2018). https://doi.org/10.1364/OL.43.002082

[73] Zi, X. Z., Wang, L. F., Chen, K. X. & Chiang, K. S. Mode-selective switch based on thermo-optic asymmetric directional coupler. *IEEE Photonics Technol. Lett.* **30**, 618–621 (2018). https://doi.org/10.1109/LPT.2018.2808466

[74] Jin, W. & Chiang, K. S. Mode switch based on electro-optic long-period waveguide grating in lithium niobate. *Opt. Lett.* **40**, 237–240 (2015). https://doi.org/10.1364/OL.40.000237

[75] Jin, W. & Chiang, K. S. Reconfigurable three-mode converter based on cascaded electro-optic long-period gratings. *IEEE J. Sel. Top. Quantum Electron.* **26**, 1–6 (2020). https://doi.org/10.1109/JSTQE.2020.2969568

[76] Zhang, M. R., Ai, W., Chen, K. X., Jin, W. & Chiang, K. S. A lithium-niobate waveguide directional coupler for switchable mode multiplexing. *IEEE Photonics Technol. Lett.* **30**, 1764–1767 (2018). https://doi.org/10.1109/LPT.2018.2868834

[77] Lee, B. -T. & Shin, S. -Y. Mode-order converter in a multimode waveguide. *Opt. Lett.* **28**, 1660–1662 (2003). https://doi.org/10.1364/OL.28.001660

[78] Low, A. L., Yong, Y. S., You, A. H., Chien, S. F. & Teo, C. F. A five-order mode converter for multimode waveguide. *IEEE Photonics Technol. Lett.* **16**, 1673–1675 (2004). https://doi.org/10.1109/LPT.2004.828512

[79] Riesen, N. & Love, J. D. Design of mode-sorting asymmetric Y-junctions. *App. Opt.* **51**, 2778–2783 (2012). https://doi.org/10.1364/AO.51.002778

[80] Driscoll, J. B. *et al*. .Asymmetric Y junctions in silicon waveguides for on-chip mode-division multiplexing. *Opt. Lett.* **38**, 1854–1856 (2013). https://doi.org/10.1364/OL.38.001854

[81] Feng, J., Chen, K. X., Ren, K. Y. & Chiang, K. S. Mode (de) multiplexer based on polymer-waveguide asymmetric Y-junction. in *Asia Communication and Photonics Conference* AF1G.5 (2016). https://doi.org/10.1364/ACPC.2016.AF1G.5

[82] Chen, W. W. *et al*. Silicon three-mode (de)multiplexer based on cascaded asymmetric Y junctions. *Opt. Lett.* **41**, 2851–2854 (2016). https://doi.org/10.1364/OL.41.002851

[83] Fujisawa, T. *et al*. Scrambling-type three-mode PLC multiplexer based on cascaded Y-branch waveguide with integrated mode

rotator. *J. Lightwave Technol.* **36**, 1985–1992 (2018). https://doi.org/10.1109/JLT.2018.2798619

[84] Gao, Y. *et al*. Compact six-mode (de) multiplexer based on cascaded asymmetric Y-junctions with mode rotators. *Opt. Commun.* **451**, 41–45 (2019). https://dx.doi.org/10.1016/j.optcom.2019.06.010

[85] Watanabe, T. & Kokubun, Y. Demonstration of mode-evolutional multiplexer for few-mode fibers using stacked polymer waveguide. *IEEE Photonics J.* **7**, 1–11 (2015). https://doi.org/10.1109/JPHOT.2015.2497234

[86] Dai, D. X., Tang, Y. B. & Bowers, J. E. Mode conversion in tapered submicron silicon ridge optical waveguides. *Opt. Express* **20**, 13425–13439 (2012). https://doi.org/10.1364/OE.20.013425

[87] Dai, D. X. & Mao, M. Mode converter based on an inverse taper for multimode silicon Nanophotonicsic integrated circuits *Opt. Express* **23**, 28376–28388 (2015). https://doi.org/10.1364/OE.23.028376